

Preliminary Experiment for Spectral Reflectance Estimation of Human Iris using a Digital Camera

June 8 2000

Francisco H. Imai

- 1) **Goal** – Perform preliminary experiment to check the feasibility and evaluate the accuracy of spectral estimation using a digital camera.

2) **Background**

Multi-spectral acquisition and linear methods have been widely used to estimate spectral properties of imaged materials.¹⁻²⁰

One can model multi-spectral image acquisition using matrix-vector notation. Expressing the sampled illumination spectral power distribution as

$$\mathbf{S} = \begin{pmatrix} \mathbf{s}_1 & & & 0 \\ & \mathbf{s}_2 & & \\ & & \circ & \\ 0 & & & \mathbf{s}_n \end{pmatrix},$$

(1)

and the object spectral reflectance as $\mathbf{r}=(r_1, r_2, \dots r_n)^T$, where the index indicates the set of n wavelengths over the visible range and τ the transpose matrix, representing the transmittance characteristics of the m filters as columns of \mathbf{F}

$$\mathbf{F} = \begin{pmatrix} \mathbf{f}_{1,1} & \mathbf{f}_{1,2} & \dots & \mathbf{f}_{1,m} \\ \vdots & \vdots & \vdots & \vdots \\ \mathbf{f}_{n,1} & \mathbf{f}_{n,2} & \dots & \mathbf{f}_{n,m} \end{pmatrix} \quad (2)$$

and the spectral sensitivity of the detector as

$$\mathbf{D} = \begin{pmatrix} \mathbf{d}_1 & & & 0 \\ & \mathbf{d}_2 & & \\ & & \circ & \\ 0 & & & \mathbf{d}_n \end{pmatrix}, \quad (3)$$

then the captured image is given by $\mathbf{D}_c=(\mathbf{D}\mathbf{F})^T\mathbf{S}\mathbf{r}$, where \mathbf{D}_c represents the digital counts, and the color vector can be represented as $\mathbf{c}=\mathbf{A}\mathbf{t}=(X, Y, Z)^T$ where X, Y, Z are the CIE tristimulus values. The CIELAB L^*, a^*, b^* are given by the non-linear transformation ξ , where $\xi(X, Y, Z) = L^*, a^*, b^*$.

If the spectral reflectance is sampled in the range of 400 nm to 700 nm wavelength in 10 nm intervals we have 31 samples. Ideally we should have 31 signals to

reconstruct the spectral reflectance. However, it is possible to decrease the dimensionality of the problem by performing principal component analysis on the spectral samples. Given a sample population of spectral reflectances, it is possible to identify a small set of underlying basis functions whose linear combinations can be used to approximate and reconstruct members of the population. Then the reconstructed sample \hat{r}_i is given by $\hat{r}_i = \Phi\alpha_i$, where $\Phi = (\mathbf{e}_1 \ \mathbf{e}_2 \ \dots \ \mathbf{e}_p)$ are the set of the eigenvectors (principal components) used for the estimation and the coefficients (eigenvalues) associated with the eigenvectors are $\alpha_i = (\mathbf{a}_1 \ \mathbf{a}_2 \ \dots \ \mathbf{a}_p)^T$ where the index $p \leq n$, and where n is the number of samples used to perform *a priori* principal component analysis. When the eigenvalues are arranged in descending order the fraction of variance explained by the first corresponding p vectors is

$$\mathbf{v}_p = \frac{\sum_{i=1}^p \mathbf{a}_i}{\sum_{i=1}^n \mathbf{a}_i}. \quad (4)$$

In this linear method, a set of spectral reflectances \mathbf{r} is measured and then a set Φ of eigenvectors, who explain typically more than 99.9% of the original sample, is calculated by principal component analysis. Then, the set of eigenvalues, α , is calculated by $\alpha = \Phi^T \mathbf{r}$. We know that the set of digital counts corresponding to the spectral samples can be calculated by the equation $\mathbf{D}_c = (\mathbf{D}\mathbf{F})^T \mathbf{S}\mathbf{r}$. A relationship between digital counts and eigenvalues can be established by the equation

$$\mathbf{A} = \alpha \mathbf{D}\mathbf{c}^T [\mathbf{D}\mathbf{c}\mathbf{D}\mathbf{c}^T]^{-1} \quad (5)$$

The matrix \mathbf{A} can be used to calculate the eigenvalues α_i from digital counts to reconstruct the spectral reflectance. Here, it is important to notice that the number of channels should equals the number of eigenvectors used in the system.

An *a priori* measurement of the representative samples of my target universe, using spectroradiometry/spectrophotometry, followed by digital camera imaging of the same samples gives me data to calculate the transformation matrix of Eq. (5). This transformation matrix can be used for further spectral estimation of objects of the same universe.

Using these linear method tools it is possible to extend the colorimetric characterization of the human iris by Melgosa et.al.²¹ to a spectral characterization.

3) *Experiment*

Instruments:

Topcon SL-7E ophthalmic microscope (serial 1705194)

This instrument shown in Figure 1 provided by Prof. William Fisher at the biomedical photographic laboratory at RIT is a very precise instrument where it is possible to attach digital cameras and spectroradiometers and it provides sufficient magnification to image/measure particular spots on the iris. It also provides interface with a monitor and possibility to record videos for documentation purposes.

More information can be obtained at <http://www.topcon.com/MEDICAL/SL7E.htm>.



Figure 1. Topcon SL-7E slit lamp ophthalmic microscope

Kodak DCS 620 – provided by Prof. William Fischer

This camera shown in Figure 2 is a very fast 2 MB digital camera (1728 by 1168 pixels) that uses Nikon F5 Camera body with 12 bit dynamic range and photometrically linear data. More information can be found at:

<http://www.kodak.com/global/en/professional/products/cameras/dcs620/dcs620Index.shtml>



Figure 2. Kodak DCS 620 digital camera.

PhotoResearch PR-650 SpectroScan Spectroradiometer -

This spectroradiometer shown in Figure 3 has 128 diode-array, Pritchard optical system, and samples with spectral range from 380 to 780 nm with 8 nm bandwidth and accuracy of 2nm. This instrument operates with batteries and records data using a 256 K card (approximately 169 measurements) and output using a RS-232 to PC. More information can be obtained at <http://www.photoresearch.com/brochures/650/650.pdf>



Figure 3. PhotoResearch PR-650 Spectro Scan Spectroradiometer

Targets:

- a) Small Color Checker based on GretagMacbeth ColorChecker shown in Figure 4.



Figure 4. Mini Color Checker

- 2) Fake eye balls (used for ophthalmic photography practice or prosthetics)
3) Actual iris of some volunteers: F.H.I., J.W. U., E.D.M., W.,F. and students of biomedical photographic laboratory.

Procedure:

I. Illumination level and geometrical adjustments.

Illumination level and geometry should be adjusted to produce non-saturated images with good S/N ratio and a reasonable dynamic range. It can be accomplished capturing some digital images and checking the histogram in 12 bits. The illumination and geometry also should allow sufficient signal for reliable measurements using the spectroradiometer. Once the system is adjusted, the geometrical features, such as position, distance should be recorded to reproduce the adjustment in future sessions.

II. Verification of the spectral measurement accuracy through the Topcon Microscope system.

The spectral reflectances of the ColorChecker and fake eye balls are measured using the SpectroScan spectroradiometer directly and through the microscope using same geometry/illumination to verify if the optics is introducing distortions in our measurements.

III. Making control images to relate spectral measurements with digital counts.

A high-resolution digital picture of the entire area of the iris of each subject is captured and printed. This print will give a way to track the spots that are measured by the spectroradiometer. Alternatively, a video signal can be recorded for the same purpose as shown in Figure 5. Some notation specifying the angle in which the image is taken also gives us a recording of the position.

IV Measurement of spectral radiance of the illuminant

A white reference is used to measure the spectral radiance of the illuminant using the SpectroScan spectroradiometer

V. Measurement of spectral radiance from spots on the iris and imaging of the same spots (or entire image) using the digital camera.



Figure 5. Video signal from the slit lamp displayed on a monitor

Measurement and Imaging:

Measurement/Imaging I

In our first visit to the biomedical photographic laboratory we choose a Carl Zeiss Inc. ZVS 1470 slit lamp ophthalmic microscope (serial 309949) shown in Figure 6 (back view) and Figure 7 (front view). The spectral radiance coming from the iris of five subjects were measured and some pictures taken using the Kodak DCS 620 (shown in Figure 8) to test the feasibility of the experiments combining the slit lamp ophthalmic microscope with the spectroradiometer and the digital camera.



Figure 6. Carl Zeiss Inc. ZVS 1470 slit lamp ophthalmic microscope. Back view showing the multiple-use attachments (for imaging/measurement)



Figure 7. Carl Zeiss Inc. ZVS 1470 slit lamp ophthalmic microscope. Front view showing chin rest and the slit lamp illumination.



Figure 8. Carl Zeiss Inc. ZVS 1470 slit lamp ophthalmic microscope with an attached Kodak DCS 620 camera.

Measurement/Imaging II

Since the images taken using the Carl Zeiss were dark and the measurements took time to complete, we solved to change the slit lamp system to the Topcon SL-7E and we could get better images (using the Kodak DCS 620 digital camera as shown in Figure 9) and measurements are performed using this new slit lamp ophthalmic microscope system. We imaged a mini color checker, a fake eye ball and real iris using the Kodak/Nikon DCS 620 (fstop 16 and ISO 640). At the same time 1 to 4 spectral radiance measurements were taken using the spectrophotometer attached to the optical system of the slit lamp. One measurement was performed for each patch of the color checker. A halon was measured under halogen, and using green and blue filtered halogen lamp. One measurement was performed and one image was taken for the fake eye ball and one measurement for 3 to 4 different position of the iris of 6 subjects were taken along with one image for each position.



Figure 9. Topcon SL-7E slit lamp ophthalmic microscope with an attached Kodak DCS 620 camera.

Figures 10a, 10b and 10c show three different views of the Kodak DCS 620 digital camera and the SpectraScan spectroradiometer attached to the Topcon SL-7E slit lamp ophthalmic microscope during the imaging and measurement of a mini color checker.



Figure 10a. Measurement and Imaging of a mini color checker (rear view). **Figure 10b.** Measurement and Imaging of a mini color checker (view from the top).



Figure 10c. Measurement and Imaging of a mini color checker (frontal view).

The imaging and measurements were performed under halogen lamp (with two layers of paper with a diffuser property to minimize the specular reflection on the eye as shown in Figure 11).



Figure 11. Diffuser paper in front of the halogen illumination.

Figure 12 shows the iris of a subject (David Curtis) being photographed by Prof. William Fisher while Joe Unander measure the spectral radiance.

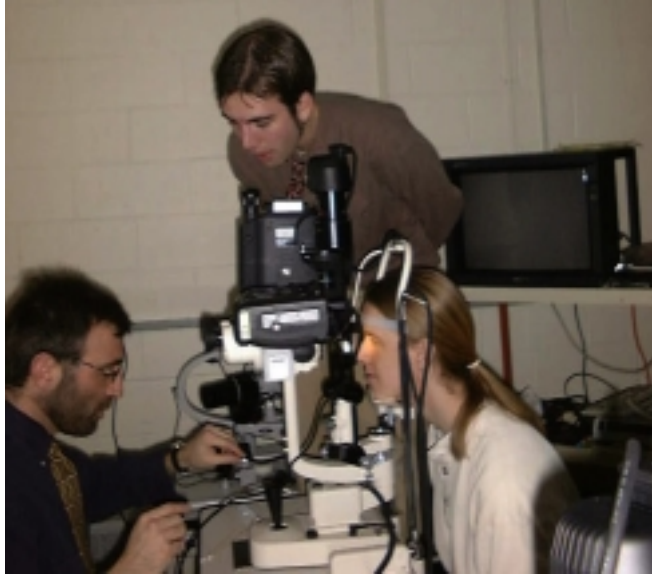


Figure 12. Imaging and measurement session

Measurement III

The spectral radiance measurements of the previous session were partially repeated for the same slit lamp (Topcon SL-7E serial 1705194), the same imaging geometry using halogen lamp with diffusing paper. However this time, the spectral measurements were made without the magnification of the optical system to check if the slit lamp optical system is introducing significant error or not in the spectral radiance measurements. The mini color checker, halon and four position of the iris of two subjects were measured and recorded.

4) Analysis and Discussion

A) Spectral Radiance of the halogen lamp with diffuser

The spectral radiance of the halogen lamp (with diffuser) was calculated from both the measurements through the optical path and without the optical path using the white patch of the mini color checker. The plot comparing both measurements is shown in Figure 13. Figure 14 shows the difference in spectral radiance between both calculated values. The spectral radiance factor rms error between the calculations was approximately 0.001. It is possible to see that there was a difference in using or not the optical system of the slit lamp ophthalmic microscope but the difference was not very significant and it might be the result of the fact the measurements were performed in different days (although the geometry was carefully set up, it was not a perfect reproduction of the previous measurement).

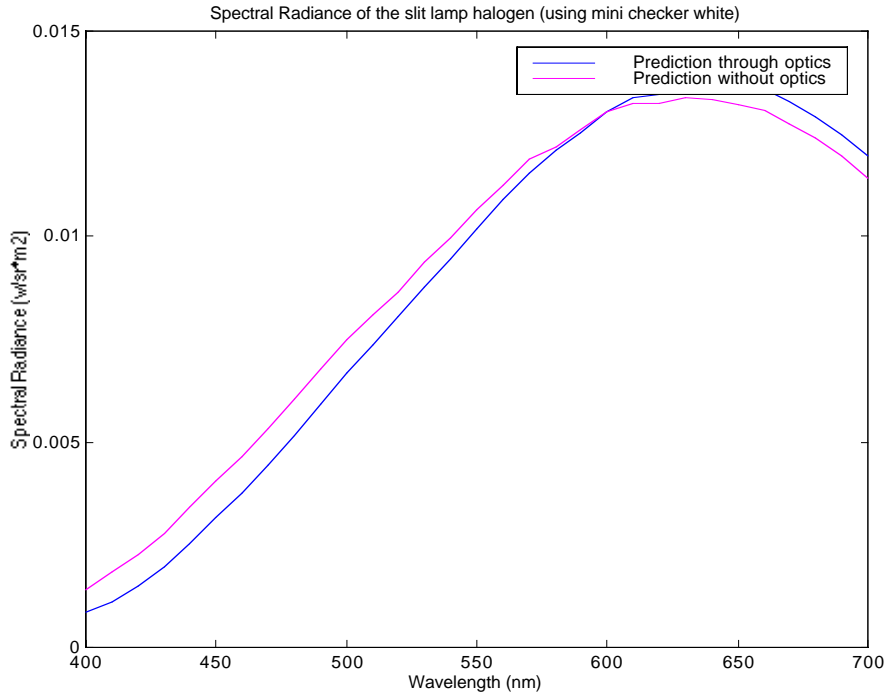


Figure 13. Comparison between calculated spectral radiance of the diffused halogen lamp through the optical system and without the optical system.

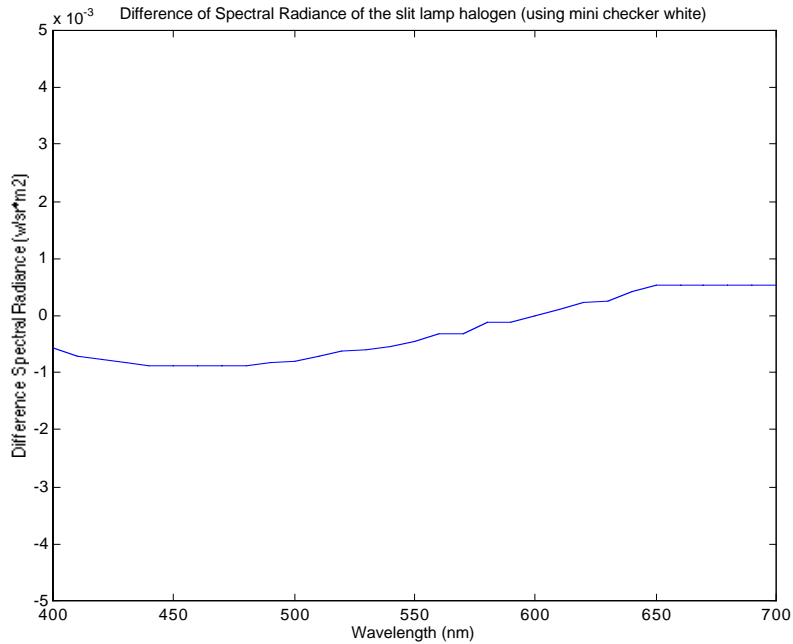


Figure 14. Difference in spectral radiance between calculated spectral radiance of the diffused halogen lamp through the optical system and without the optical system.

2) Estimation of the spectral radiance of filtered halogen lamp

Figure 15 shows a comparison of the calculated spectral radiances of the unfiltered halogen lamp of the slit lamp and the filtered lamp using green and blue filters that is part of the Topcon SL-7E system. The measurements were performed using the white patch of the mini color checker without the optical system of the ophthalmic microscope.

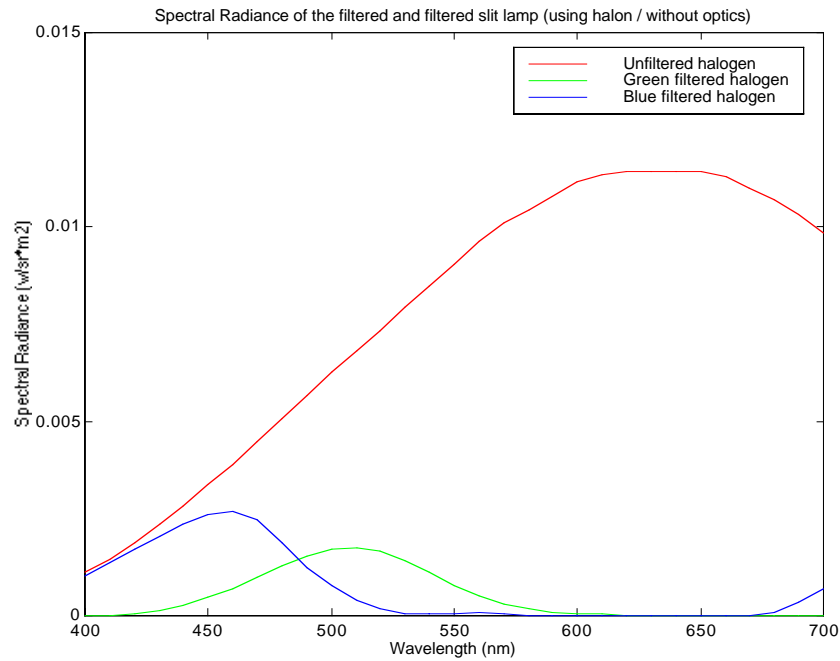


Figure 15. Comparison of the spectral radiance of the unfiltered halogen lamp and the filtered halogen lamp using blue and green filters.

It is possible to notice that the transmittance of the filters used by the Topcon slit lamp is quite low and different alternatives using Kodak Wratten filters should also be considered if more than 3 channels (R, G, B without filtering) is necessary.

Figure 16 shows a comparison between calculated spectral radiance of the diffused halogen lamp with green filter through the optical system and without the optical system. The spectral radiance factor rms error between the calculations was approximately 0.001. It is possible to see that although there is a slight difference the calculation gives a very good match even for calculations using low signals.

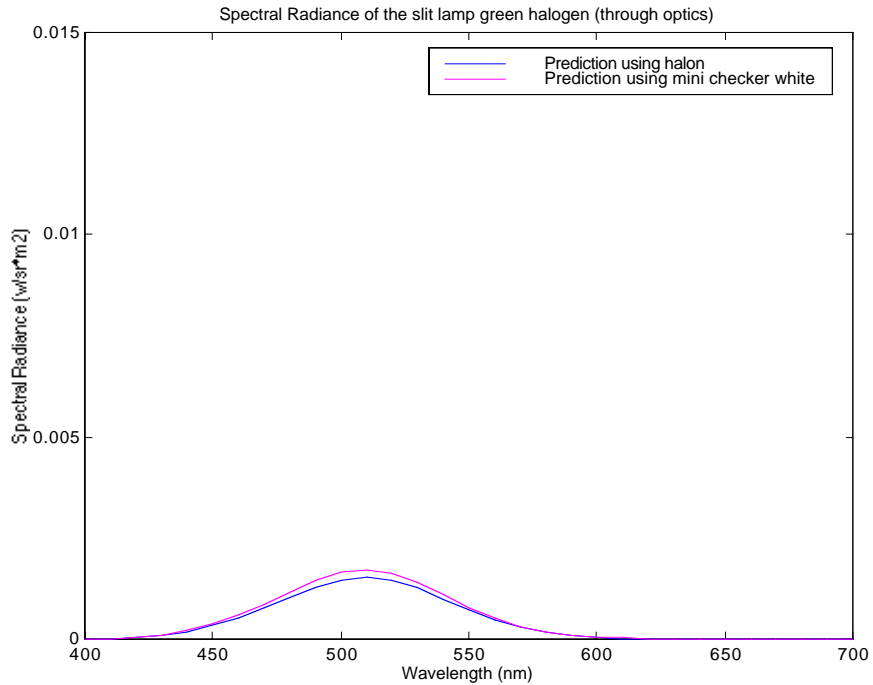


Figure 16. Comparison between calculated spectral radiance of the diffused halogen lamp with green filter through the optical system and without the optical system.

C) Estimation of the spectral reflectances of the mini color checker using the measurement through the optical system of the slit lamp.

Using the spectral radiance calculated in the previous section, the spectral reflectance of the mini color checker was calculated and shown in Figure 17. Figure 18 shows the difference in spectral reflectance between the measured and the calculated spectral reflectances. The average spectral reflectance factor rms error between the calculations was approximately 0.028. The spectral reflectances of the mini color checker were measured using a Gretag SPM 60 spectrophotometer (45/0).

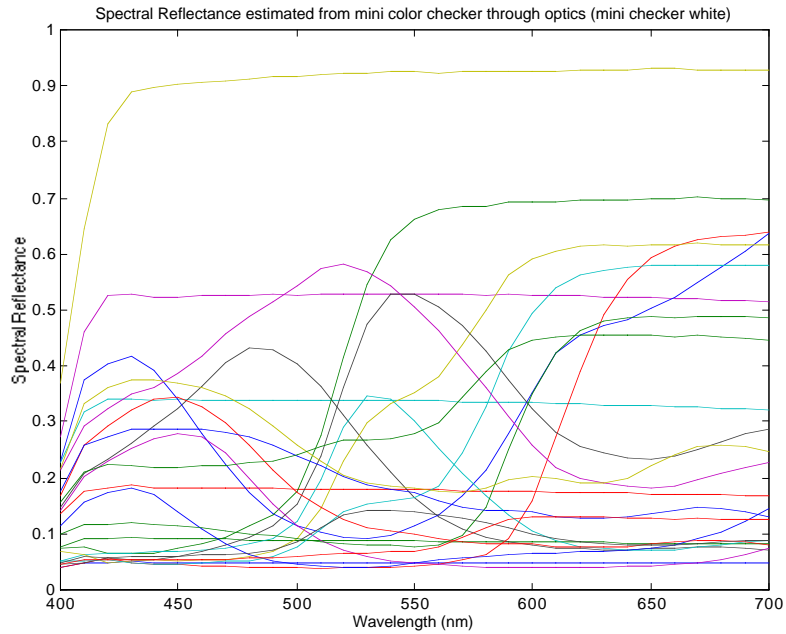


Figure 17. Calculated spectral reflectance of the mini color checker.

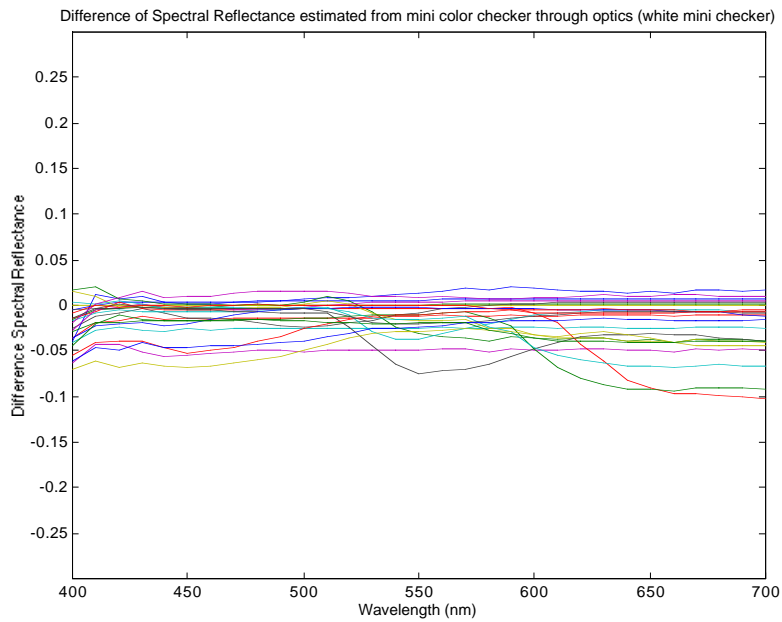


Figure 18. Difference between calculated and measured spectral reflectance of the mini color checker

D) Kodak DCS 620 photometric linearity

Since linear methods will be applied to reconstruct the spectral reflectance from the digital counts it is necessary to check the photometric linearity of the Kodak DCS 620 raw data. The 12 bit raw data provided by the Kodak DCS 620 was obtained using the

Photoshop Kodak DCS Acquire 5.6.3 plug-in. Then, each image was saved as 16 bit TIFF and processed using IDL 5. 2 in SGI environment. Each of the 24 mini color patches taken under both halogen lamp and filtered halogen lamp using green filter was cropped in the same position and the values in the cropped area were averaged. Figure 19, 20 and 21 show the plot of the lightness (Y) under D50 illuminant and 1931 observer of the gray scale of the mini checker in function of the averaged digital counts, respectively for red, green and blue channels. The linear fit R^2 were 0.989, 0.996 and 0.996 respectively for red, green and blue channels. It is possible to conclude that the camera is giving photometric linear response.

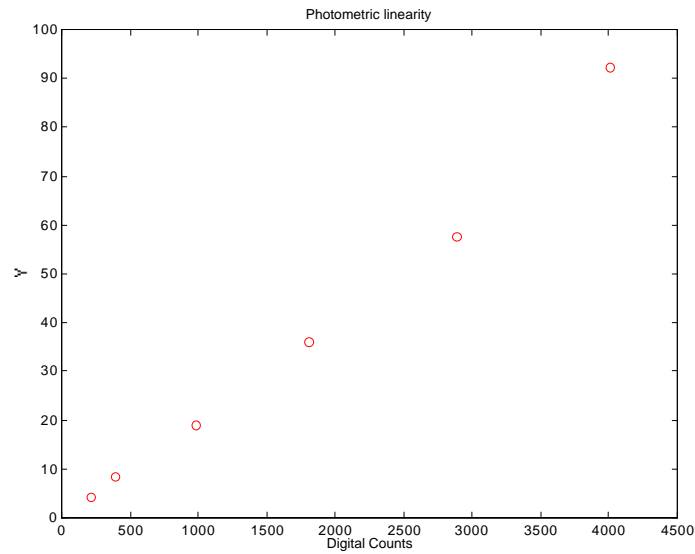


Figure 19. Photometric linearity of the red channel

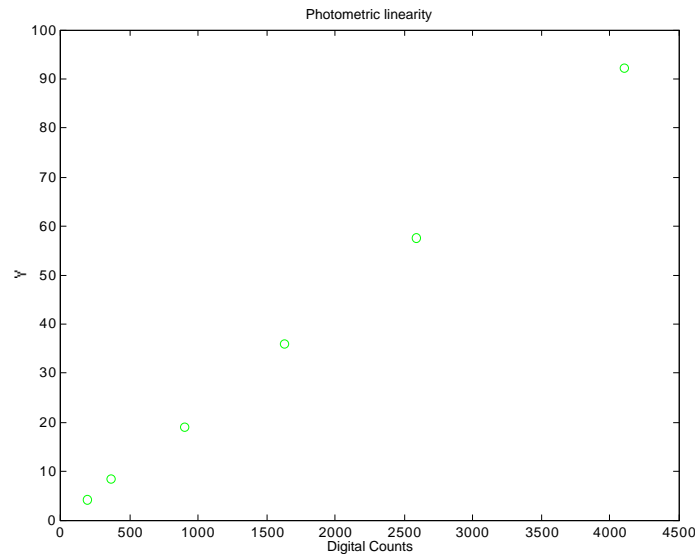


Figure 20. Photometric linearity of the green channel.

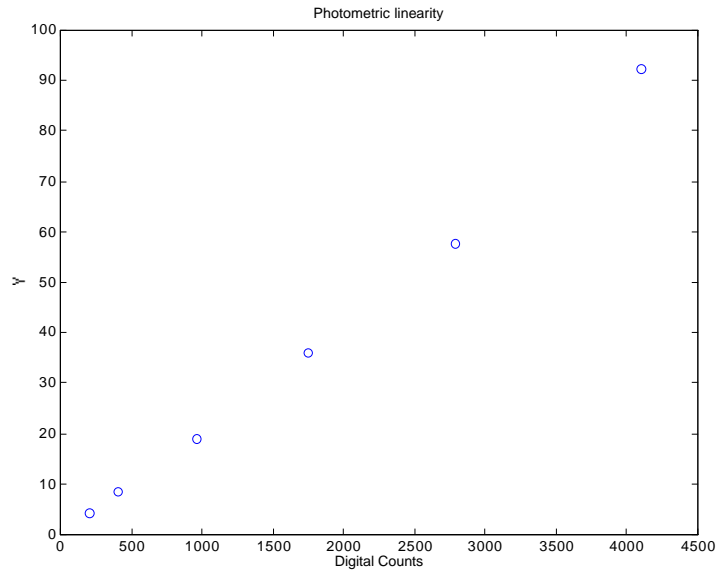


Figure 21. Photometric linearity of the blue channel

E) Spectral reflectance estimation of the mini color checker using 6 digital signals and eigenvectors from the sampled data.

Principal component analysis was performed using the measured values of the spectral reflectance factors for the mini color checker. The principal components are shown in Figure 22.

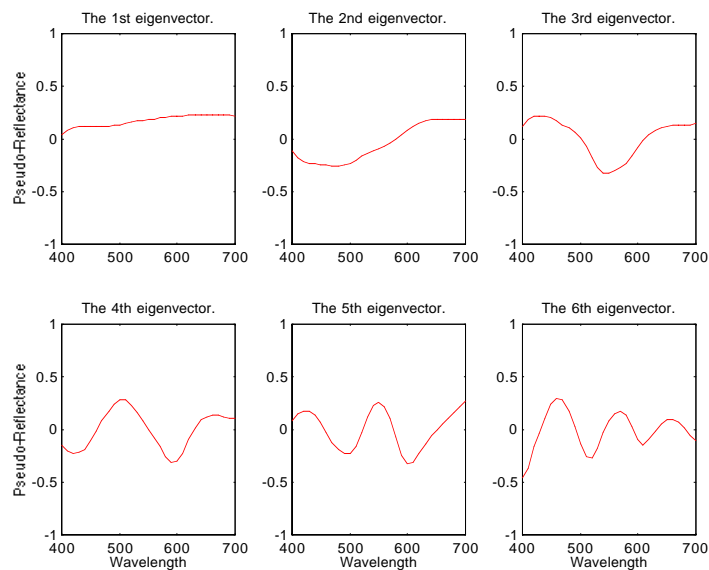


Figure 22. First to Sixth principal components of the mini color checker reflectance.

Figure 23 gives the cumulative proportion index graph for the mini color checker. It is possible to see that 4 to 6 eigenvectors can theoretically reconstruct very well the original spectral reflectances.

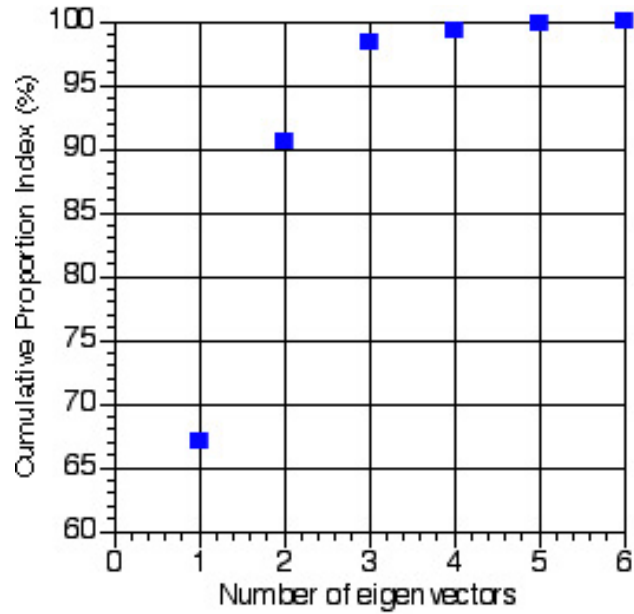


Figure 23. Cumulative proportion index graph for the mini color checker eigenvectors.

Figure 24 shows the ΔE^*_{94} (D50, 1931 observer) histogram for the colorimetric accuracy between the measured values and the estimation using the eigenvectors.²²

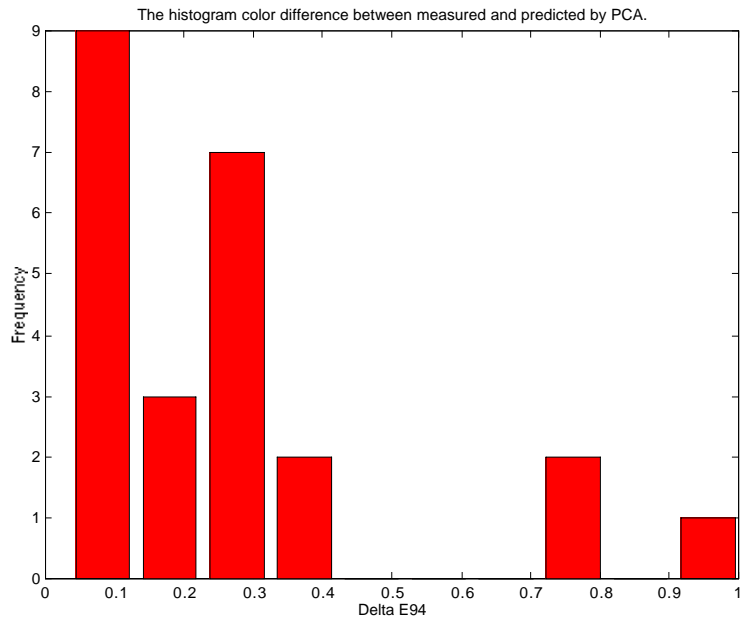


Figure 24. ΔE^*_{94} histogram between measured and estimated values using six eigenvectors.

The colorimetric and estimated spectral reflectance values using eigenvectors are presented at Table I. The metameric index was calculated using the Fairman metameric black method, between standard illuminants D50 and A using ΔE^*_{94} in the calculations.²³

Table I. Colorimetric and spectral accuracy between measured and estimated spectral reflectance values using six eigenvectors.

Value	ΔE^*_{94} (AD501931)	Spectral reflectance factor rms error	Metameric Index (D50, A, 1931) (ΔE^*_{94})
Average	0.3	0.012	0.1
Standard deviation	0.3	0.004	0.1
Maximum	1.0	0.018	0.4
Minimum	0.0	0.003	0.0

Six channels (RGB values under unfiltered halogen and RGB values under halogen with green filter) were used in conjunction with the spectral eigenvectors and a 6 by 6 transformation matrix was generated:

$$A = \begin{bmatrix} 2.7 & -12.4 & -1.4 & 28.1 & 0.4 & 13.4 \\ 6.1 & -40.2 & 2.7 & -21.9 & -10.4 & 31.8 \\ 0.5 & 30.9 & -6.5 & 24.5 & 4.5 & -5.5 \\ 2.7 & -40.7 & -3.7 & 49.8 & -3.3 & 11.5 \\ -1.0 & 131.8 & -5.3 & 50.0 & 4.8 & -43.9 \\ 0.8 & -53.4 & 2.6 & -24.0 & -3.0 & 24.2 \end{bmatrix} \quad (6)$$

Figure 25 shows the ΔE^*_{94} histogram between measured and estimated values from six digital counts using the matrix represented in Equation 6 and the *a priori* calculated eigenvectors. Table II summarizes the colorimetric and spectral accuracy.

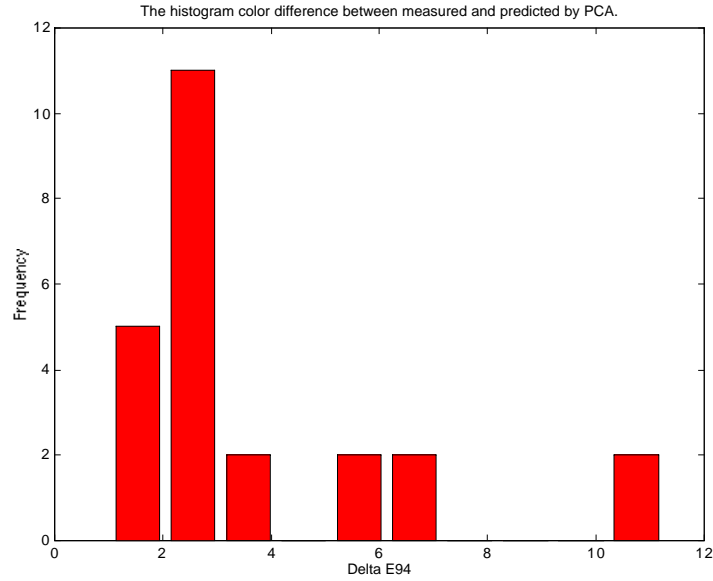


Figure 25. ΔE^*_{94} histogram between measured and estimated values from six digital counts using the matrix represented in Equation 6 and the *a priori* calculated eigenvectors.

Table II. Colorimetric and spectral accuracy between measured and estimated spectral reflectance values from six digital counts using the matrix represented in Equation 6 and the *a priori* calculated eigenvectors.

Value	ΔE^*_{94} (D50,1931)	Spectral reflectance factor rms error	Metameric Index (D50, A, 1931) (ΔE^*_{94})
Average	3.7	0.027	0.5
Standard deviation	2.7	0.011	0.5
Maximum	11.3	0.056	2.1
Minimum	1.0	0.012	0.0

From Figure 25 and Table II it is possible to observe that although the average colorimetric and spectral accuracy values were reasonable some patches produced bad results. It is due to the fact that the signals obtained using green-filtered halogen lamp for the darker patches were very low producing a very unstable transformation matrix shown in Equation 6. It enforces the belief that a better way to change the illumination is necessary.

F) Spectral reflectance estimation of the iris using three digital signals and eigenvectors from the sampled data.

The imaged iris were also acquired in 12 bits, cropped at the same position for the images acquired using the same orientation (for instance, for all the images acquired at 9 o'clock the same area was cropped) and the values inside the cropped area were averaged for each channel. Figure 26, 27, and 28 shows some examples of imaged iris (in this case 8 bit gamma corrected data was used just as illustrations for this report) and their corresponding measured spectral radiances.

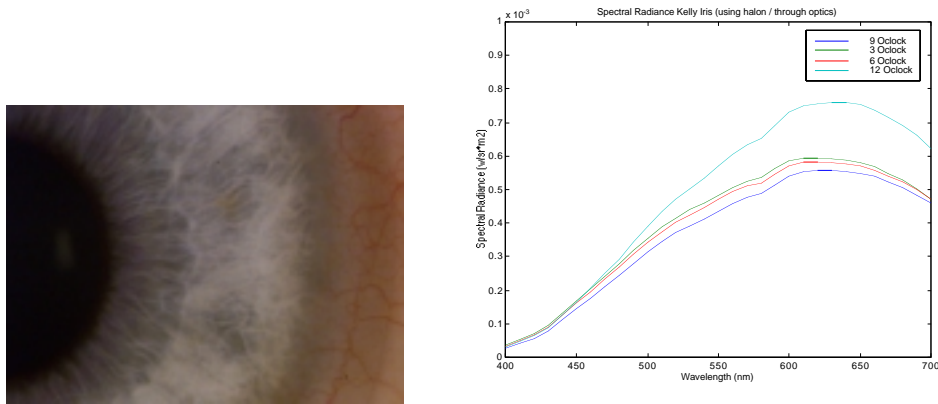


Figure 26. Light blue iris image and corresponding measured spectral radiances.

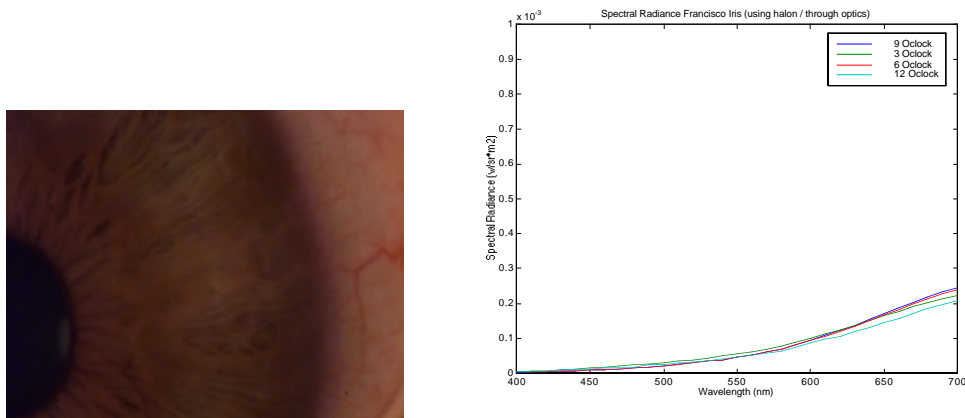


Figure 27. Dark brown iris image and corresponding measured spectral radiances.

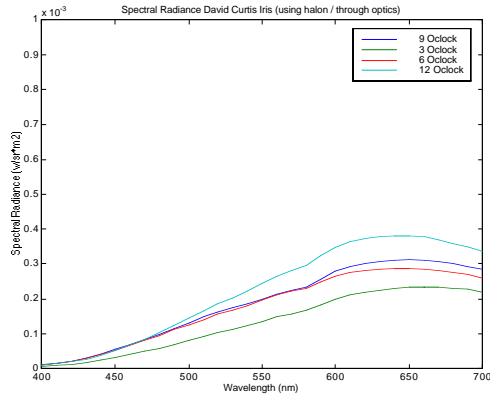


Figure 28. Green iris image and corresponding measured spectral radiances.

The spectral reflectance factors of the measured area in the iris were estimated from the measured spectral radiances and the calculated spectral radiance of the halogen illumination of the slit lamp. Principal component analysis was performed using the estimated values of the spectral reflectance factors for the iris. The principal components are shown in Figure 29.

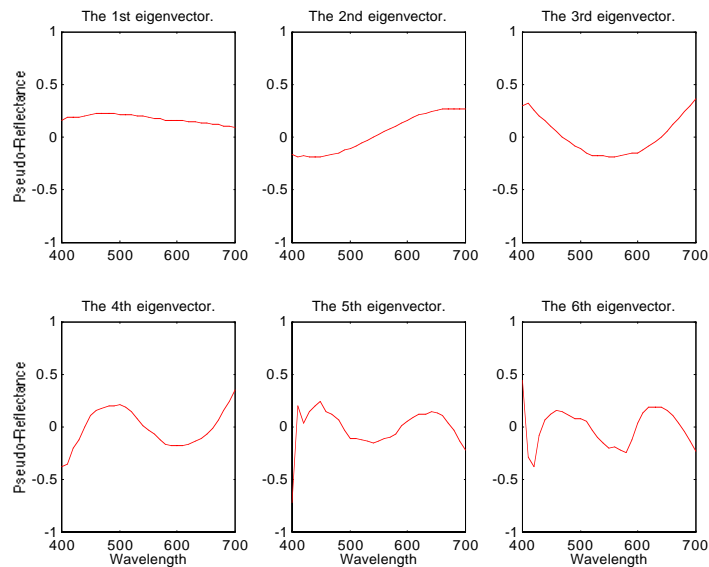


Figure 29. First to Sixth principal components of the iris spectral reflectance.

Figure 30 gives the cumulative proportion index graph for the iris spectral reflectance eigenvector analysis. It is possible to see that 3 to 4 eigenvectors can theoretically reconstruct very well the original spectral reflectances.

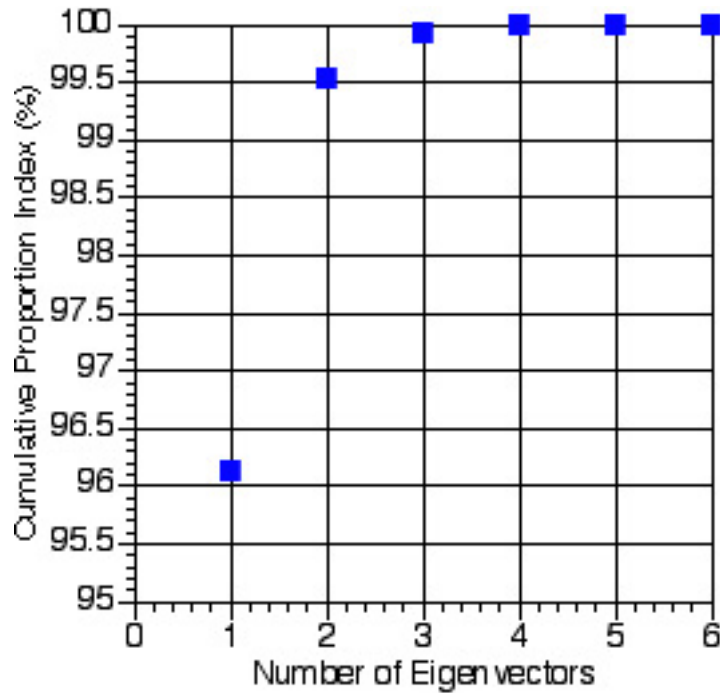


Figure 30. Cumulative proportion index graph for the iris eigenvectors.

Since only three channels per image were available (no iris pictures were taken under green filtered light because it produced very dark and noisy images) only three eigenvectors, corresponding to the three R, G, B signals were used in the estimation. Figure 31 shows the ΔE^*_{94} (D50, 1931 observer) histogram for the colorimetric accuracy between the measured values and the estimation using the eigenvectors.

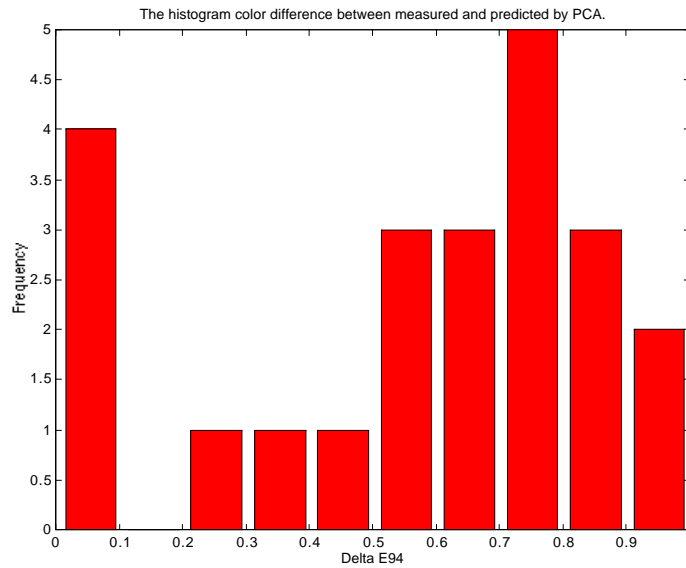


Figure 31. ΔE^*_{94} histogram between measured and estimated values using three eigenvectors.

The colorimetric and estimated spectral reflectance values using three eigenvectors are presented at Table III.

Table III. Colorimetric and spectral accuracy between measured and estimated spectral reflectance values using three eigenvectors.

Value	ΔE^*_{94} (D50,1931)	Spectral reflectance factor rms error	Metameric Index (D50, A, 1931) (ΔE^*_{94})
Average	0.6	0.001	0.0
Standard deviation	0.3	0.000	0.0
Maximum	1.0	0.002	0.1
Minimum	0.0	0.000	0.0

Three channels (RGB values under unfiltered halogen) were used in conjunction with the spectral eigenvectors and a 3 by 3 transformation matrix was generated:

$$A = \begin{bmatrix} -0.5 & 1.5 & 0.9 \\ 1.8 & -0.03 & -1.6 \\ 0.3 & -0.6 & 0.4 \end{bmatrix} \quad (7)$$

Figure 32 shows the ΔE^*_{94} histogram between measured and estimated values from three digital counts using the matrix represented in Equation 7 and the *a priori* calculated eigenvectors. Table IV summarizes the colorimetric and spectral accuracy.

Table IV. Colorimetric and spectral accuracy between measured and estimated spectral reflectance values from three digital counts using the matrix represented in Equation 7 and the *a priori* calculated eigenvectors.

Value	ΔE^*_{94} (D50,1931)	Spectral reflectance factor rms error	Metameric Index (D50, A, 1931) (ΔE^*_{94})
Average	3.3	0.003	0.7
Standard deviation	3.5	0.001	2.3
Maximum	12.4	0.006	11.1
Minimum	0.0	0.001	0.0

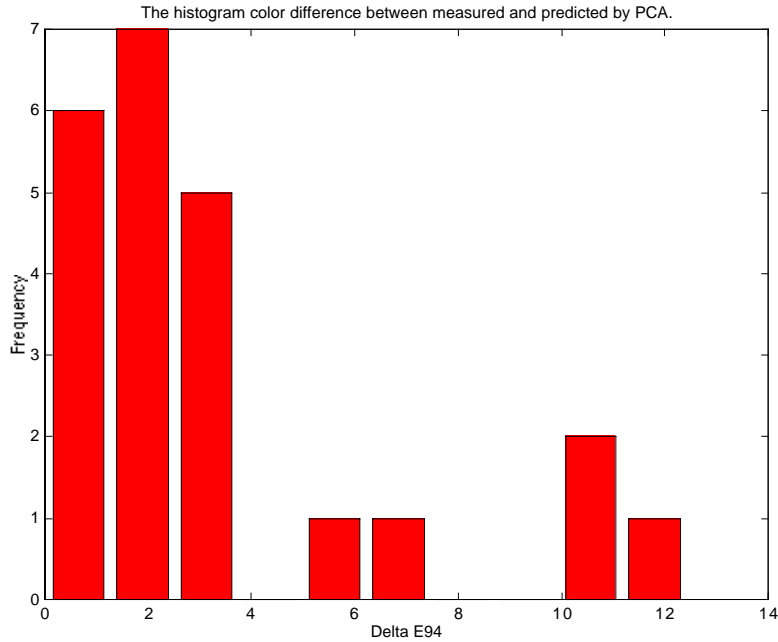


Figure 32. ΔE^*_{94} histogram between measured and estimated values from three digital counts using the matrix represented in Equation 7 and the *a priori* calculated eigenvectors.

Although the results of the estimation from digital counts to spectral reflectance were generally satisfactory, it produces some bad estimations. Analyzing the images corresponding to the bad colorimetric accuracy it is found that all the images were pictures of darker iris colors and they were either unfocused or with specular reflections (as shown in Figure 33) in the measured/averaged areas that lead to the estimation error.

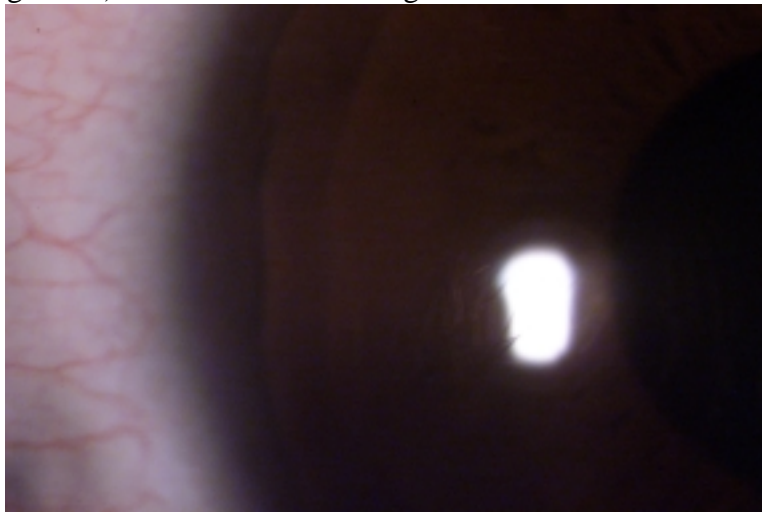


Figure 33. Example of an image with a specular reflection of the illumination in the spot of measurement and averaging of the digital counts.

Please, note that the transformation shown in Equation 6 and 7 are effective only for the particular system and geometry used in the experiments.

4) *Generation of a spectral image of the human iris*

The transformation matrix shown in Equation 7 was used to generate a spectral image. To visualize the spectral image under one arbitrary illuminant and observer, the spectral radiance of daylight D50 standard illuminant and 2 degree observer were used to generate the XYZ tristimulus values. Then, Bradford transformation was used to convert from D50 white point to D65 (white point of a CRT display available in the laboratory) and a sRGB transformation was applied. Finally a gamma of 1.8 was applied before generating the RGB rendering of the spectral image. Figure 34 shows a rendered spectral image. The generated image was darker than expected and it can be related to the calibration procedure during the spectral radiance measurements.



Figure 34. Rendered picture of the iris from its spectral image

5) *Conclusion and Future Work*

Preliminary experiments were conducted to show the feasibility of retrieving the spectral reflectance of human iris from the signals of a digital camera. This method uses statistical analysis (principal component analysis) and a linear method relating the weights of the eigenvectors to the digital counts. Spectral radiance measurements and imaging were performed through a Slit lamp ophthalmic microscope that provides magnification of the human iris. Preliminary experiments showed that although the optical system can alter the measurements the error is not significant if the system is well calibrated and geometrically stable. To insure that this method works, the photometric linearity of the system must be checked. Preliminary results showed that this method is a powerful tool to generate a spectral image of the human iris.

Some issues to be addressed:

- 1) Spatial white correction. - Although two diffuser papers were used in front of the halogen lamp to improve the uniformity of the illumination, the illumination was not perfectly uniform. A possible way to improve this is to performing white spatial correction using some white ball with the shape and geometry of the human eye.
- 2) New imaging geometry – It was observed that specular reflections can be a hazard to perform accurate estimation. New imaging geometries can lead to less presence of unwanted highlights.
- 3) Creation of a database of iris spectral reflectance measurements and images – Due to the limitations in the access of the imaging system as well as limited number of subjects it was not possible to build a comprehensive database. Any future work trying to improve and extend this method should consider building this database.
- 4) Although the iris spectral estimation was performed using only three signals, more channels should be considered to improve accuracy. Instead of using the filters build-in the slit lamp, Wratten absorption filters can give us better transmittance and therefore better signals to produce multiple sets of R, G, B digital signals.
- 5) More light sensitive image device – A more sensitive imaging device also can be considered to get better signal/noise and consequently improve the estimations.

Acknowledgements: I would like to thanks Prof. William Fisher of the biomedical photography, Photographic Department, R.I.T. for his guidance and for allowing us to use the installations in his laboratory. I also would like to thank Joe Unander for his help. I would like to thank for the patience of the many students who participated in the experiments in the experiments at the biomedical imaging laboratory.

References

1. F. H. Imai and R. S. Berns, High-resolution multi-spectral image archives: A hybrid approach, *Proc. of The Sixth Color Imaging Conference: Color Science, Systems, and Applications*, 224 (1998).
2. R. S. Berns, F. H. Imai, P. D. Burns and Di-Y. Tzeng, Multi-spectral-based color reproduction research at the Munsell Color Science Laboratory, *Proc. of SPIE Europto Series 3409*, 14 (1998).
3. R. S. Berns, Challenges for color science in multimedia imaging, in L. MacDonald and M. R. Luo, Eds., *Colour Imaging: Vision and Technology*, John Wiley & Sons, Chichester, 1998, pp. 99-127.
4. F. H. Imai and R. S. Berns, Spectral Estimation Using Trichromatic Digital Cameras, *Proc. of the International Symposium on Multispectral Imaging and Color Reproduction for Digital Archives*, 42 (1999).

5. F. H. Imai and R. S. Berns, A comparative analysis of spectral reflectance reconstruction in various spaces using a trichromatic camera system, *Proc. of The Seventh Color Imaging Conference: Color Science, Systems, and Applications*, 21 (1999).
6. J. Y. Hardeberg, H. Brettel, and F. Schmitt, Spectral characterization of electronic cameras, *Proc SPIE Europto Series* **3409**, 100 (1998).
7. H. Maitre, F. J. M. Schmitt, J-P. Crettez, Y. Wu and J. Y. Hardeberg, Spectrophotometric image analysis of fine art paintings, *Proc. IS&T/SID Fourth Color Imaging Conference: Color Science, Systems and Applications*, 50 (1996).
8. S. Baronti, A. Casini, F. Lotti and S. Porcinai, Multispectral imaging system for the mapping of pigments in works of art by use of principal-component analysis, *Applied Optics* **37**, 1229 (1998).
9. F. K nig, Reconstruction of natural spectra from a color sensor using nonlinear estimation methods, *Proc. IS&T s 50th annual conference*, 454 (1997).
10. F. K nig and W. Pr fke, The practice of multispectral image acquisition, *Proc. SPIE* **3409**, 34 (1998).
11. W. Pr fke, Analysis-synthesis transforms versus orthogonal transforms for coding reflectance spectra, *Proc. IS&T/SID 5th Color Imaging Conference: Color Science, Systems and Applications*, 177 (1997).
12. W. Pr fke, Transform coding of reflectances spectra using smooth basis vectors, *J. Imaging Sci. Technol.* **40**, 543 (1996).
13. Y. Miyake, Y. Yokoyama, N. Tsumura, H. Haneishi, K. Miyata and J. Hayashi, Development of multiband color imaging systems for recording of art paintings, *Proc. SPIE* **3648**, 218 (1999).
14. H. Haneishi, T. Hasegawa, N. Tsumura and Y. Miyake, Design of color filters for recording artworks, *IS&T s 50th Annual Conference*, 369 (1997).
15. S. Tominaga, Spectral Imaging by a Multi-Channel Camera, *Proc. of SPIE* **3648**, 38 (1999).
16. M. J. Vrhel and H. J. Trussel, Color correction using principal components, *Color Res. Appl.* **17**, 328 (1992).
17. M. J. Vrhel, R. Gershon and L. S. Iwan, Measurement and analysis of object reflectance spectra, *Color Res. Appl.* **19**, 4 (1994).
18. D. S. S. Vent, *Multichannel analysis of object-color spectra*, Master Degree Thesis, Rochester Institute of Technology, 1994.
19. P. D., Burns, *Analysis of image noise in multi-spectral color acquisition*, Ph. D. Thesis, Rochester Institute of Technology, 1997.
20. P. D. Burns and R. S. Berns, Error propagation analysis in color measurement and imaging, *Color Res. Appl.* **22**, 280, (1997).
21. M. Melgosa, M. J. Rivas, L. G mez and E. Hita — Towards a colorimetric characterization of the human iris, *Ophtal. Physiol. Opt.*, to be published in 2000.
22. CIE, Publication No. 116, *Industrial Colour-Difference Evaluation*, Commission Internationale de l'clairage, Vienna, Austria, (1995).
23. H. S. Fairman, Metameric correction using parameric decomposition, *Color Res. Appl.*, **12**, 261-265 (1997).